The M waves of the biceps brachii have a stationary (shoulder-like) component in the first phase: Implications and recommendations for M-wave analysis

The M waves of the *biceps brachii* have a stationary (shoulder-like) component in the first phase: implications and recommendations for M-wave analysis

Javier Rodriguez-Falces[1], **Alberto Botter**[2,3], **Taian Vieira**[2,3] and **Nicolas Place**[4]

1 Department of Electrical and Electronical Engineering, Public University of Navarra, Pamplona, Spain
2 Laboratory for Engineering of the Neuromuscular System (LISiN), Department of Electronics and Telecommunication, Politecnico di Torino, Torino, Italy
3 PoliToBIOMed Lab, Politecnico di Torino, Turin, Italy
4 Institute of Sport Sciences, University of Lausanne, Lausanne, Switzerland
E-mail: javier.rodriguez.falces@gmail.com
Keywords: compound muscle action potential, M wave, end-of-fiber signals, non-propagating components, muscle excitability, muscle-fiber length, volume conduction

Abstract

Objective. We recently documented that compound muscle action potentials (M waves) recorded over the 'pennate' *vastus lateralis* showed a sharp deflection (named as a shoulder) in the first phase. Here, we investigated whether such a shoulder was also present in M waves evoked in a muscle with different architecture, such as the *biceps brachii*, with the purpose of elucidating the electrical origin of such afeature. *Approach*. M waves evoked by maximal single shocks to the brachial plexus were recorded in monopolar and bipolar configurations from 72 individuals using large (10 mm diameter) electrodes and from eight individuals using small (1 mm diameter) electrodes arranged in a linear array. The changes in M-wave features at different locations along the muscle fiber direction were examined. *Main results*. The shoulder was recognizable in most (87%) monopolar M waves, whereas it was rarely observed (6%) in bipolar derivations. Recordings made along the fiber direction showed that the shoulder was a stationary (non-propagating) feature, with short duration (spiky), which had positive polarity at all locations along the fibers. The latency of the shoulder (9.5 ± 0.5 ms) was significantly shorter than the estimated time taken for the action potentials to reach the biceps tendon (12.8 ms). *Significance*. The shoulder must be generated by a dipole source, i.e. a source created at a fixed anatomical position, although the exact origin of this dipole is uncertain. Our results suggest that the shoulder may not be due to the end-of-fiber signals formed at the *biceps brachii* tendon. The shoulder is not related to any specific arrangement of muscle fibers, as it has been observed in both pennate and fusiform muscles. Being a stationary (non-propagating) component, the shoulder is not reliable for studying changes in sarcolemmal excitability, and thus should be excluded from the M-wave analysis.

1. Introduction

Knowledge of the electrical formation (electrogenesis) of the compound muscle action potential (M wave) is essential in research and clinical practice, as many techniques are based on the analysis of the M-wave waveform (Rodriguez-Falces and Place 2018a). Despite its extensive use, there is no full understanding of the way in which the shape of the M wave is determined by the electrical activity in the muscle. A simplified description of the M-wave biphasic shape assumes that the M-wave first phase results from the propagation of action potentials along the muscle fibers, whereas the second phase is thought to reflect the extinction of these action potentials at the tendon (Lateva *et al* 1996). According to this simplified view, the M-wave first phase would be formed by *propagating* components, whilst the second phase would be composed of *non-propagating* (end-of-fiber) signals. Such simplistic characterization of the M wave, however, may be erroneous and misleading since the electrical formation of the M wave is influenced by many biological factors ranging from anatomical and physiological aspects to architectural and biophysical properties of the muscle (Keenan *et al* 2006, Rodriguez-Falces and Place 2018a).

In a recent study performed in the *vastus lateralis* (Rodriguez-Falces and Place 2018b), we showed that most M waves recorded monopolarly over the innervation zone showed a 'deflection' or shoulder-like feature in the descending portion of the first phase (for examples, see figure 1). This 'protuberance' or shoulder was also observed in the *tibialis anterior* M waves by Thomas *et al* (1989), although the authors did not investigate the electrical origin of this feature. In our previous work, we used recordings along the muscle fiber direction to demonstrate that the shoulder had a non-propagating character (Rodriguez-Falces and Place 2018b). This means that non-propagating components determine not only the second phase of the M wave, but also the final part of the first phase (i.e. the shoulder). The importance of identifying the parts of the M wave formed by stationary (non-propagation) components is that these components are not valid for studying changes in sarcolemmal excitability. The reason is that stationary signals are highly sensitive to changes in muscle architectural properties (Rodriguez-Falces and Place 2018a). To date, the shoulder-like feature has only been observed in pennate muscles (*vastus lateralis* and *tibialis anterior*) and whether or not it is present in muscles with a different architecture has not been tested.

The exact origin of the electrical source causing the shoulder remains to be elucidated. Various possible origins have been proposed (Rodriguez-Falces and Place 2018b). One plausible electrical explanation is end-of-fiber signals generated at the tendon of the same muscle where the M wave is recorded. Indeed, because the individual constituents of an M wave are dispersed in time, the propagating component of some fibers inevitably overlaps with the non-propagating component of other fibers. Thus, it is possible that some non-propagating components might significantly 'contaminate' the first phase of the M wave, and that this contamination is revealed by the presence of a 'hump' (shoulder) in the first phase. Another possible origin of the shoulder is end-of-fiber signals generated from nearby muscles, i.e. cross-talk contamination. This explanation would be feasible if the stimulated nerve trunk innervates various muscles located in close proximity to each other, as is the case in the muscles innervated by the femoral nerve and brachial plexus.

It has also been suggested that the origin of the shoulder may be related to the specific architecture of pennate muscles (Rodriguez-Falces and Place 2018b). In the in-depth pennate architecture, due to the inclination of the fibers relative to the skin surface, surface potentials have a more localized spatial distribution (Mesin *et al* 2011). In the case of M waves, such localized spatial distribution implies that the time distance between the maximum of the 'propagating' component and the end-of-fiber component is reduced, which may favor the appearance of the shoulder in the M-wave first phase. Another reason why the shoulder may be a unique feature of pennate muscles is that, in these muscles, the recording electrode may be placed over the superficial aponeurosis, which means that the electrode would lie just above the 'origin point' of some fibers. With such electrode-fiber spatial disposition, the 'profile' of the generated end-of-fiber signals may be such that it gives rise to the appearance of a shoulder in the M wave. Whereas the above considerations are reasonable, it must be noted that in the *vastus lateralis* the superficial aponeurosis coversonly its proximal two-thirds (Toia *et al* 2015): however, in our previous studies the recording electrodes were placed over the distal third of the *vastus lateralis* (Rodriguez-Falces and Place 2018b). Thus, our electrodes were likely not located over the superficial aponeurosis, but were lying parallel to the most superficial (and distal) muscle fibers. This observation questions whether the shoulder is a feature specific to pennate muscles.

The objectives of the present study were: (1) to determine whether the shoulder-like feature is present in M waves evoked in a fusiform muscle, such as the *biceps brachii*, and (2) to clarify the electrical origin of such feature. Based on the arguments presented above, we hypothesized that the shoulder is not related to a specific muscle architecture, and thus this feature may be present in M waves recorded in the *biceps brachii*. The study included recordings along the fiber's direction to precisely assess the electrical character of the different features of the M wave. This study was designed to gain a deeper understanding of the electrical formation of the M wave, with a view to establishing which portion of the M wave truly reflects electrical activity propagating under the electrode.

2. Material and methods

2.1. Organization of the study and participants

Analysis of the shoulder in the *biceps brachii* comprised three main steps: (1) comprehensive observation of all M waves to determine whether certain shapes (profiles) were repeated; (2) identification of the propagating and non-propagating components of the M wave by observing the changes in the M-wave

profile at different sites along the fiber's direction; (3) examination of how the different features of the M wave changed as stimulation intensity was increased from subthreshold to supramaximal levels.
M-wave recording was performed using two different electromyography (EMG) detection systems. The first detection mode utilized surface electrodes with a large (10 mm diameter) recording surface (see figure 2). These electrodes were chosen as they are widely used in sport science and clinical neurophysiology. With these large-area electrodes, M waves were collected from 72 participants who volunteered in previous studies from our laboratory. Participants (59 men, 13 women) were aged between 22 and 39 years (mean ± SD: 27 ± 5 years). Their average height and mass were 178 ± 5 cm and 70 ± 5 kg, respectively.
The second EMG detection system involved the use of a high-density surface EMG array, which contained 16 electrodes with a small (1 mm diameter) recording surface. With these small-area electrodes, M waves were collected from eight participants (two women), aged between 23 and 39 years (31 ± 5 years). Their average height and mass were 176 ± 5 cm and 72 ± 5 kg, respectively.
All volunteers gave their informed consent to the experiments. The study was approved by the Ethics Committee of the Public University of Navarra. For both EMG detection systems, M waves were plotted with negative voltages upward (figure 1). Thus, the terms 'positive' and 'negative' were used with reference to the direction on the plot, rather than the true electrical polarity.

2.2. Experimental setup

Experiments were performed on the *biceps brachii* and consisted of evoking maximal M waves while the muscle was at rest. Participants were comfortably seated with the arm flexed at 60 ◦ (with 0 ◦ being the full extension) and the forearm vertical and supinated, while the hand held an adjustable handle connected to the strain gauge. The shoulder-trunk angle was 90 ◦ in the sagittal axis. Extraneous movements of the arm and hand were prevented by Velcro straps. Before testing, the skin over the *biceps brachii* muscle was prepared by light abrasion with sandpaper and cleansing with rubbing alcohol.

2.3. Identification of the muscle fiber's direction and innervation zone

The methods utilized to locate the innervation zone and the muscle fiber's direction were common for the two EMG detection systems described above. Specifically, a *dry* linear array of 16 electrodes (5 × 1 mm, 5 mm inter-electrode distance) was placed along the longitudinal axis of the *biceps brachii* (short head). The array was connected to a multichannel amplifier (OT Bioelettronica, Torino; bandwidth 10–500 Hz), and EMG signals were detected in a single differential configuration during low-level voluntary contractions. The direction of the muscle fibers was identified by choosing the orientation of the array that resulted in the optimal propagation of action potentials (Farina *et al* 2002). Such a direction was marked on the skin with a waterproof felt-tip pen. The main innervation zone was located by identifying the EMG channel(s) that had minimum amplitude or phase reversal (Masuda *et al* 1985).

2.4. M-wave recordings

Two different EMG detection systems were employed to record M waves. In the first detection mode (figure 2), M waves were recorded using three circular self-adhesive Ag/AgCl electrodes (Kendall Meditrace 100, Tyco, Canada). The electrodes had a large recording area (10 mm diameter) and were positioned with an inter-electrode distance of 20 mm. The electrodes were arranged in a belly–tendon configuration, as depicted in figure 2(a). The 'belly' electrodes were placed over the short head of the *biceps brachii*, longitudinally along the muscle fiber's direction. The 'tendon' (reference) electrodes were connected together and placed on the flexor retinaculum of the wrist. The ground electrode was placed adjacent to the tendon electrode. To standardize the electrode positioning in all participants, the belly electrodes were placed relative to the innervation zone of the *biceps brachii* as follows. The most proximal electrode was always located above the innervation zone (IZ) and was referred to as mono-IZ. The other two electrodes, mono-D1 and mono-D2, were placed adjacent to each other, on the distal side of the innervation zone, as shown in figure 2(a). The belly–tendon M waves, as depicted here, can be considered as monopolar M waves since the tendon (reference) electrode was placed on an electrically non-active site of the body (Tucker and Türker 2005). In addition to these monopolar potentials, M waves were derived in a bipolar configuration by subtracting monopolar M waves from pairs of adjacent electrodes. Using the above electrode settings, the Bip-D1 and Bip-D2 M waves were obtained in the proximal-to-distal direction, as depicted in figure 2(a).
In the second EMG detection system, M waves were recorded using a 16-channel linear electrode array

with small contact surfaces (1 × 1 mm) and small inter-electrode distances (5 mm). The linear array was oriented along the muscle fiber's direction (see above). The array was located so that its eighth electrode coincided with the position of the innervation zone. To ensure proper electrode–skin contact, the electrode cavities of the array were filled with conductive paste. The surface EMG signals were amplified, filtered and digitalized by a multichannel amplifier (see below for details, EMG-USB, OT Bioelettronica, Torino, Italy). A reference electrode strap was moistened and wrapped around the subject's dominant wrist.

2.5. Brachial plexus stimulation

The brachial plexus was stimulated using a rectangular (35 × 45 mm) self-adhesive electrode (cathode) positioned on the supraclavicular fossa, whereas the anode (35 × 45 mm) was placed on the acromion (Smith *et al* 2007). Single rectangular pulse stimuli of 0.1 ms duration were delivered by a high-voltage constant current stimulator (model DS7AH; Digitimer, Hertfordshire, UK). The maximal stimulus intensity was determined by gradually increasing the stimulation intensity until a plateau in the M-wave amplitude was observed. This level of intensity was then further increased by 20% to ensure that the stimulation remained supramaximal throughout the experimental session.

2.6. Data analysis

EMG signals from the large electrodes were detected with the MP150 amplifier (5000 Hz sampling rate, 10–750 Hz bandwidth, 100 amplification factor, BIOPAC, Goleta, CA, USA), recorded with a commercially available software (AcqKnowledge, Biopac Systems, Goleta, CA, USA), and subsequently exported to MATLAB (version R2012b; The Math-Works, Natick, MA, USA) for quantitative analysis. EMG signals from the array of electrodes were detected with a multichannel amplifier (2048 Hz sampling rate, 10–750 Hz bandwidth, 100 amplification factor; EMG-USB; OTBioelettronica and LISiN, Politecnico di Torino, Italy), and recorded with a MATLAB script (version R2012b; The Math-Works, Natick, MA, USA), written specifically for the real-time visualization and acquisition of EMGs.

For the mono-IZ, mono-D1, and mono-D2 M waves, the latency of the shoulder ($Latency_{SHOULDER}$), positive peak ($Latency_{POS\text{-}PEAK}$), and negative peak ($Latency_{NEG\text{-}PEAK}$) were measured (see figure 2(c)). The starting point for the latency parameters was determined by a deviation greater than two standard deviations (SDs) from the baseline noise. The end point for the $Latency_{POS\text{-}PEAK}$, $Latency_{NEG\text{-}PEAK}$, and $Latency_{SHOULDER}$ was defined in correspondence with the positive peak, negative peak, and shoulder of the M wave, respectively. Unless otherwise stated, only the most proximal bipolar M wave (Bip-D1) was considered for analysis. Precise determination of the shoulder-like feature was performed using the method described previously (Rodriguez-Falces and Place 2018b).

Data of muscle fiber conduction velocity of the *biceps brachii* would allow us to determine whether the latency values of the shoulder correspond to the arrival of the action potentials at the *biceps brachii* tendons. Estimation of conduction velocity was performed by means of the linear electrode array, using the multidip approach described by Farina and Negro (2007). The multidip method is based on the use of a regression analysis of the spatial and temporal frequencies of multiple dips introduced into the EMG power spectrum through the application of a set of spatial filters (Farina and Negro 2007). The technique requires four consecutive EMG channels in which a clear propagation of motor unit potentials is seen. In our study, channels 3–6 of the electrode array were chosen. Conduction velocity was estimated during maximal voluntary contractions of 6 s. Three trials, separated by 3 min, were carried out, and the average conduction velocity of the trials were computed.

2.7. Statistics

Kolmogorov–Smirnov tests confirmed that each of the M-wave parameters analyzed in the current study was normally distributed. For the 72 participants assessed with the large (classical) electrodes, differences in the latencies of the M-wave positive peak, shoulder, and negative peak among the mono-IZ, mono-D1, and mono-D2 M waves evoked during supramaximal stimulation were examined using a one-way repeated measures ANOVA. The effect size (ES) of the mean differences was determined using Cohen's d. The 95% confidence interval (CI) of the differences from statistical tests was calculated, and data were presented in the text as means ±95% CIs. Statistical significance was defined as $P < 0.05$.

3. Results

3.1. M-wave analysis using the large (10 mm recording diameter) electrodes

Figure 3 shows representative examples of monopolar (first row) and bipolar (second row) M waves recorded over the innervation zone of the *biceps brachii*. In the majority (93%) of the mono-IZ M waves, the rising portion of the first phase did not have a constant slope; rather it increased abruptly at the beginning, then it slowed down for a short period, after which it increased steeply again until the positive peak of the M wave. As a result of this change in the slope, a distinct *shoulder-like* feature appeared in the ascending portion of the first phase (see the white-headed arrows in figure 3).

In most (87%) mono-IZ M waves, the descending portion of the first phase did not show a constant slope either. Essentially, the decrease from the peak was initially steep, but then the slope slowed down transiently for a brief period or even became positive (i.e. a hump emerged), and subsequently the decrease became steep again until the negative peak of the M wave (for examples, see figure 3). As a result, a *shoulder* was recognized in the declining first phase of M waves for most individuals. This shoulder could appear as a discontinuity in the slope (grey-headed arrows) or as a well-defined hump/peak (black-headed arrows). On the basis of the profile of the declining first phase, the mono-IZ M waves were classified into three types (for representative examples of each type, see figure 3).

In the type-I M waves, the shoulder was manifested as a slope-discontinuity point (figure 3(a)). The frequency of the appearance of these M waves was rather high, representing 24% of the total. For the type-II M waves, instead of a slope-discontinuity point, a distinct hump (peak) appeared, and thus these potentials displayed two peaks in the first phase (figure 3(b)). This typology of M wave was the one most frequently found (63%). A third type of M wave was identified in which the positive peak had a long latency, and the declining first phase had an approximately constant slope (i.e. no shoulder appeared) (figure 3(c)). These M waves represented only 13% of the total.

The bipolar M waves (second row) exhibited a wide variety of profiles, and only a few instances (6%) showed a shoulder in the transition between the positive and negative peaks. In these few bipolar M waves, the latency of the shoulder was different from that of their monopolar counterparts.

3.2. Identification of propagating and non-propagating components by changing the electrode position

To investigate the electrical origin of the shoulder-like feature, we first examined the changes in the M-wave shape at different recording sites from the innervation zone to the distal tendon (figure 4). For the type-I profile (figure 4(a)), the M waves at both the mono-IZ and mono-D1 locations showed an apparent slope-discontinuity point in the declining first phase, which had the same latency at both locations (see the vertical dashed line), reflecting the non-propagating nature of this feature. Interestingly, the shape of the potential changed noticeably from the mono-D1 to the mono-D2 location: essentially, the slope-discontinuity point of the mono-D1 M wave was transformed into the main positive peak of the mono-D2 M wave.

For the type-II profile (figure 4(b)), the M waves at the mono-IZ location showed two distinct positive peaks. As the recording site was closer to the tendon (mono-D1 and mono-D2), the first peak vanished gradually, whereas the second peak remained visible. It is worth noting that the latency of the first peak increased from the mono-IZ to the mono-D2 locations, whereas the latency of the second peak coincided for these locations (see the vertical dashed line), thus indicating the non-propagating character of this feature.

For the type-III profile (figure 4(c)), the M waves at the mono-IZ, mono-D1, and mono-D2 locations exhibited only one well-defined positive peak, followed by a steep declining phase with a roughly constant slope. Remarkably, the latency of the positive peak was the same at the different longitudinal positions from the innervation zone to the distal tendon (see the vertical dashed line), hence suggesting a non-propagating character.

The next step was to verify mathematically the non-propagating nature of the shoulder in the three types of M waves presented above, for the whole study group. For the type-I M waves, there was no difference (95% CI = −1.1 to 1.3, ES = 0.04) in the latency of the shoulder between the mono-IZ and mono-D1 M waves. Similarly, there was no difference (95% CI = −1.2 to 1.6, ES = 0.09) between the latency of mono-IZ shoulder and the latency of the mono-D2 positive peak. For the type-II M waves, no difference (95% CI = −1.2 to 1.5, ES = 0.08) was found in the latency of the shoulder between the mono-IZ and mono-D2 M waves. For the type-III M-waves, there was no difference (95% CI = −0.9 to 1.2, ES = 0.06) in the latency

of the positive peak between the mono-IZ and mono-D2 M waves. On the other hand, there was no difference in the latency of the final negative peak of the M waves recorded at the mono-IZ, mono-D1, and mono-D2 locations (table 1), this being true for all types of M waves.

3.3. Identification of propagating and non-propagating components by increasing stimulation intensity

To further investigate the electrical origin of the shoulder-like feature, M waves were examined at different stimulation intensities to study how propagating and non-propagating components emerged in the M wave as stimulus strength increased. As representative examples, we show in figure 5 sets of M waves evoked at three submaximal stimulation intensities for two participants, each set comprising M waves recorded along the fiber's direction. In the first participant, for Istim = 20 mA (figure 6(a)), a slope-discontinuity point can be recognized in the mono-IZ and mono-D1 M waves. As stimulation intensity increased (from 20 to 30 mA, figures 6(b) and (c)), the slope-discontinuity point of these potentials was transformed into a second positive peak. Interestingly, when plotting together the mono-IZ potentials evoked at different stimulation intensities (figure 5(d)), it can be seen that the shoulder (non-propagating component) and the first positive peak (propagating component) increased in amplitude at different rates. In the second participant, a visual distinction can easily be made between the propagating (first peak) and non-propagating (second peak)components of the M wave for all stimulation intensities (figures 6(e)–(g)). Indeed, the second peak of themono-IZ, mono-D1, and mono-D2 potentials coincided in latency at Istim = 25, 27, and 29 mA. Again,when comparing the mono-IZ potentials evoked at different stimulation intensities (figure 5(h)), it becomesclear that the amplitude of the second peak increased more than the first peak.

3.4. M-wave analysis using the electrode array

Figure 6 shows a representative example of monopolar M waves recorded with the linear electrode array, at different positions along the direction of *biceps brachii* fibers. The M waves exhibited two main positive peaks. The second peak, corresponding to the shoulder, appeared at the same latency irrespective of the distance from the electrode to the innervation zone, this being true in both the distal (plot a) and proximal (plot b) directions. It is worth noting that, in the electrodes above or close to the innervation zone (5–10), the first peak was clearly more prominent than the second one; however, as the M wave was recorded away from the innervation zone, the first peak gradually vanished, whereas the second peak became the main peak of the potential (see channels 1–3 and 11–13). This pattern of changes in the M-wave waveform was recognized in the eight individuals assessed with the electrode array. There was no difference (95% CI = −1.3 to 1.9, ES = 0.09) in the latency of the shoulder between the mono-IZ M wave recorded with the linear array (9.7 ± 0.6 ms) and the mono-IZ M wave recorded with the large electrodes (9.5 ± 0.5 ms).

3.5. Estimation of muscle fiber conduction velocity

Muscle fiber conduction velocity was estimated during maximal voluntary contractions using the linear electrode array. The estimated values of conduction velocity were 4.3 ± 0.7 m s^{-1}.

4. Discussion

Previous research has detected the presence of a 'shoulder-like' feature in the M waves recorded in pennate muscles (Thomas *et al* 1989, Rodriguez-Falces and Place 2018b). However, interpretation of the M-wave shape in pennate muscles is complex: therefore, here we selected a simpler 'model' (i.e. muscle with fusiform architecture) with the purpose of elucidating the electrogenesis of such a feature. The main findings were: (1) the shoulder was recognized in most (87%) of the monopolar M waves, whereas it was rarely found (6%) in bipolar M waves; (2) the shoulder was a non-propagating feature which had the same latency at different distances from the innervation zone; (3) the shoulder had positive polarity at all locations along the fibers; (4) the amplitudes of the main positive peak and the shoulder increased at different rates with increasing stimulation intensity. Consideration will first be given to the different manifestation of the shoulder in monopolar and bipolar M waves. Subsequently, the electrical character and origin of the shoulder were discussed, together with its practical implications.

4.1. The shoulder-like feature in the descending portion of the M-wave first phase for monopolar and bipolar M waves

Two distinct shoulders, one in the rising portion of the M-wave first phase, the other in the descending portion of the same phase, were recognized in most monopolar M waves detected over the innervation zone.

The second shoulder is the subject matter of the present study (as its electrogenesis is not well established), and thus it will be discussed more extensively below. As found in our previous study (Rodriguez-Falces and Place 2018b), the shoulder in the descending portion of the first phase could be manifested in two forms: (1) as a deflection during which the slope changes considerably, thereby leading to a slope-discontinuity point), or (2) as a deflection that gives rise to a distinct peak. In the *vastus lateralis*, the first form of the shoulder (slope-discontinuity point) was more frequently found (76% of the total) than the second one (24%), whereas in the *biceps brachii* the opposite occurred, and the majority of M waves (63%) displayed a distinct peak in the declining first phase.

Interestingly, in the *biceps brachii* a third type of shape (profile) was identified (13% of the total) in which the shoulder was apparently absent, and the monopolar M wave exhibited only one well-defined positive peak with an unusually long latency. This type-III waveform could be interpreted as a variation of the type-II waveform, in which the 'missing' first peak had blurred into the ascending first phase and the existing long-latency peak is actually what we called a 'shoulder'. Support for this interpretation comes from our experiments with varying stimulation intensity (participant #34 in figure 5), where it was observed that, as stimulation intensity increased, the first peak gradually vanished (to the point of disappearing at the supramaximal stimulus intensity), while the second became the main (and, in fact, only) peak of the potential.

As for the bipolar M waves, although they showed a wide range of waveforms, in general they had a constant-slope transition between the positive and negative peaks, i.e. no shoulder was visible. Moreover, in the few instances where a shoulder was present in the bipolar M wave, it did not coincide in latency with the shoulder of the corresponding monopolar M wave. The absence of the shoulder in the bipolar M waves is likely due to the common mode rejection introduced by the bipolar electrode configuration: this electrode arrangement would largely remove the far-field (volume-conducted) potentials generated by dipole sources (Tucker and Türker 2005). Finally, our observations seem to be in agreement with previous experimental observations in the *biceps brachii*, since, in those studies in which a monopolar electrode configuration was adopted, the shoulder was visible (Zijdewind *et al* 2006, Nuzzo *et al* 2016), whereas this feature was missing in studies where the bipolar mode was utilized (L´ev´enez *et al* 2008, Klass *et al* 2008).

4.2. The electrical character of the shoulder-like feature

Our M-wave recordings provide convincing evidence that the shoulder-like feature has a non-propagating character. First, inspection of the M waves obtained with the large (10 mm recording diameter) electrodes revealed that: (1) for the type-I waveform, the slope-discontinuity point lying in the declining first phase had the same latency at the mono-IZ, mono-D2, and mono-D1 locations; (2) for the type-II waveform, the second peak of the potential occurred at the same latency at different recording sites along the fiber direction. It could be argued that this non-propagating behavior of the shoulder is partly due to the signal averaging introduced by the large electrodes, known to exert a smoothing (low-pass filter) effect on the potential (van Dijk *et al* 2009), and that such a non-propagating response would not be observed in M-wave recordings made by smaller electrodes. However, our M-wave signals recorded with the 1 mm diameter electrodes of the array demonstrated that this is not so; indeed, these potentials exhibited a shoulder that had the same latency irrespective of the electrode distance to the innervation zone (for an example, see figure 6). Additional indirect evidence supporting the 'standing' character of the shoulder-like feature comes from our experiments involving graded electrical stimulation, in which the first peak (propagating component) and the shoulder (non-propagating component) of the M wave augmented in amplitude at different rates, thus reflecting the different electrical content and nature of these two parts of the M wave.

4.3. The electrical origin of the shoulder-like feature

The non-propagating (standing) character of the shoulder indicates that this component must be generated by a 'stationary' electrical source, i.e. a source created at a fixed anatomical position. Such characteristics correspond unequivocally to a dipole source (Dumitru and King 1991). Indeed, dipole sources are created when the travelling action potential encounters inhomogeneities or 'disturbances' in the geometry, size, or conductivity of the volume conductor (Kimura *et al* 1984, Stegeman *et al* 1997). Such a description includes not only dipoles created at the fiber–tendon junction during the extinction of the action potentials, but also dipoles created due to a change in the geometry (curvature) along the course of a muscle/nerve fiber or to alterations in the conductivity/morphology of the extracellular medium. Therefore, our search for the origin

of the shoulder-like feature should not be limited to end-of-fiber signals, but rather the search should be open to 'all' dipole-field components.

It could be argued that the shoulder-like feature is due to end-of-fiber signals arising at the fiber–tendon junctions of the muscle where the M wave is recorded. However, various objections can be raised against this possibility. First, the shoulder observed in the present M waves is composed by 'positive' electrical activity, whereas the end-of-fiber components of the mono-IZ, -D1, and -D2 M waves were 'negative' (precisely speaking, the M-wave final phase, formed by the sum of temporally dispersed end-of-fiber components, was negative). When the electrode is placed above the innervation zone of a fusiform muscle (as our mono-IZ electrode), the bioelectricity theory anticipates that the end-of-fiber potentials are recorded with negative polarity (Rodriguez-Falces *et al* 2012), consistent with the M-wave final phase. Second, the end-of-fiber component (i.e. the final phase) of the *biceps brachii* M wave is clearly longer in time (i.e. wider) than the spiky shoulder-like feature. A third (more mathematical) argument can be made by comparing the latency observed for the shoulder, around 9–10 ms (table 1), with the expected time taken for the action potentials to reach the ends of the fibers in the *biceps brachii*. Our estimated values of muscle conduction velocity were 4.3 ± 0.7 m s $^{-1}$ (similar to those measured by previous authors such as Prutchi 1995, Lange *et al* 2002), and the estimates of the fascicle length of the *biceps brachii* at an elbow flexion angle of 60 $^{\circ}$ are on average 110 mm (Nelson *et al* 2016, 2018). Thus, assuming a fiber semilength of 55 mm, this implies that action potentials would take 12.8 ms to reach the biceps tendon. This time of propagation is clearly longer than the latency of the shoulder (9–10 ms). Whereas the above arguments seem well-founded, classic dogmas of volume conductor theory have shown some limitations and inaccuracies (Dumitru and King 1991), and thus the possibility that end-of-fiber effects are somehow involved in the shoulder should not be excluded completely.

Another explanation for the shoulder could be end-of-fiber components generated by an 'interfering' muscle innervated by the same nerve as the *biceps brachii*. These components would be recorded in the *biceps brachii* by virtue of volume conduction, i.e. cross-talk. This explanation resolves some of the objections described above. For example, the end-of-fiber potential generated by the interfering muscle may be recorded in the target muscle with positive polarity, depending on the relative position between the recording electrode and the interfering muscle (Dumitru and King 1991). As for the short latency of the shoulder (9–10 ms), this could be explained by the short muscle fibers of the 'interfering' muscle (*brachialis, coracobrachialis, triceps*, among others).

The shoulder-like feature may be due to dipole-field components other than the end-of-fiber signals. In fact, the stationary peaks recognized in somatosensory evoked potential experiments cannot be due to the termination of action potentials at the tendons (Cracco and Cracco 1976, Yamada *et al* 1985, Kameyama *et al* 1988). Rather, these non-propagating peaks are generally attributed to the passage of the nerve action potential volley along certain disturbing sites on the 'long' pathway from the stimulation site to the brain. In the present experiments, we can only speculate that the shoulder may be due to: (1) changes in the geometry (curvature) along the course of nerve or muscle fibers; (2) alterations in the conductivity/morphology of the volume conductor (Stegeman *et al* 1997); and (3) changes in the diameter of nerve or muscle fibers (Ounjian *et al* 1991).

In our previous study in the *vastus lateralis*, we suggested the possibility that the shoulder may be a feature specific to pennate muscles (Rodriguez-Falces and Place 2018b). Specifically, two arguments were provided. First, in the pennate architecture surface potentials have a more localized spatial distribution (Mesin *et al* 2011), which would increase the likelihood that the end-of-fiber signals contaminate the propagating component of the M-wave. The second consideration is that, in pennate muscles, if the recording electrode is lying above the superficial aponeurosis, the extinction of action potentials at this aponeurosis may generate a shoulder component in the M wave. These two arguments, however, are ruled out by the present observations that the shoulder also appears in the M waves recorded from a fusiform muscle. Therefore, the physical arrangement of muscle fibers cannot be an explanation for the shoulder.

4.4. Practical implications and recommendations

Implications of the present work fundamentally apply to M waves recorded in monopolar configurations. Thus, our results are of relevance for studies performed in the *biceps brachii* as many groups adopted the belly–tendon (monopolar) electrode configuration when targeting this muscle (Cupido *et al* 1996, McFadden and McComas 1996, Calder *et al* 2005, Zijdewind *et al* 2006, Hunter *et al* 2016), although the bipolar electrode arrangement is also utilized (L´ev´enez *et al* 2008, Riley *et al* 2008, Booghs *et al* 2012). First of all, the

present findings will help to distinguish between the propagating and non-propagating parts of a monopolar M wave. Specifically, we showed that only the initial portion of the M-wave first phase, comprised between the onset and the shoulder-like feature, can be regarded as having a propagating character; the final (remaining) portion of the M wave (which includes the shoulder and the negative phase) is composed of non-propagating signals. Then, the shoulder-like feature provides an unequivocal landmark to discriminate between the parts of the M wave corresponding to the propagating and non-propagating events. This is of paramount importance as only the propagating content can be expected to reliably reflect the changes in sarcolemmal membrane excitability (Rodriguez-Falces *et al* 2015). For this reason, identification of the shoulder-like feature must be incorporated as a routine in the M-wave analysis of future studies.
Our results support the recommendation that, if the belly–tendon (monopolar) configuration is to be used, the belly electrode should be placed above (or close to) the innervation zone (Rodriguez-Falces 2016). Indeed, it has been shown that, only when the belly electrode is located around (±20 mm) the innervation zone, does the monopolar M wave have an initial portion (comprised between the onset and the shoulder-like feature) formed by propagating content. As the belly electrode approaches the biceps' proximal and/or distal tendons (for example, at the mono-D2 location in figure 4), the first phase of the M wave is more and more contaminated by non-propagating components, and thus this M wave is not valid for the assessment of membrane excitability. The practice of placing the active electrode above the innervation region has been utilized in several muscles such as the *biceps brachii* (Hunter *et al* 2016), *tibialis anterior* (Thomas *et al* 1989), and *abductor pollicis* (Bigland-Ritchie *et al* 1982). Nevertheless, we advise the belly–tendon (monopolar) configuration to be used preferentially for studies focused on understanding the electrical formation of the M wave. However, if the purpose of the study is to examine changes in sarcolemmal excitability (that occur during fatigue, for example), then the electrodes should be placed in a bipolar configuration, since the common mode rejection introduced by the bipolar electrode configuration largely removes the volume-conducted (stationary) potentials, as demonstrated in the present study.

4.5. A note on the shoulder-like feature in the rising portion of the M-wave first phase

The initial steep rising edge observable in the mono-IZ M waves is due to the standing wave generated during the initiation of the action potentials at the innervation zone (Lateva *et al* 1996). After this initial rapid increase, the slope of the rising phase slowed down markedly, once the two depolarized zones have been fully formed. This abrupt change in the slope gives rise to a distinct shoulder-like feature in the rising phase. Whereas this shoulder is blurred and/or inconsistently found in the mono-IZ M waves recorded in some muscles (quadriceps*, tibialis anterior,* thenar muscles), it is particularly well-defined in the *biceps brachii* and appears in practically all M waves of this muscle.

5. Conclusions

In summary, we found that most (87%) of the monopolar M waves recorded over the innervation zone of the *biceps brachii* exhibited a 'shoulder-like' feature in the descending portion of the first phase. Such a shoulder was rarely found (6%) in M waves recorded bipolarly. Recordings made along the fiber's direction unequivocally showed that the shoulder was a non-propagating feature, occurring at the same latency at all recording sites. We, therefore, conclude that the shoulder must be generated by a dipole source, known to be created at a fixed (stationary) anatomical position. However, the exact origin for the dipole could not be elucidated. The observations made for the shoulder (positive polarity at all recording sites, spiky shape, and a latency shorter than the time taken for the action potentials to reach the biceps tendon) suggest that this feature may not be due to end-of-fiber signals formed at the tendon of the *biceps brachii*. Additionally, it has been demonstrated that the shoulder is not related to any specific arrangement of muscle fibers, since this feature has been observed in both pennate (*vastus lateralis*) and fusiform (*biceps brachii*) muscles. Future studies, which include motor-point stimulation of the muscle, are needed to further investigate the involvement of end-of-fiber signals and cross-talk in the shoulder generation.

References

Bigland-Ritchie B, Kukulka C G, Lippold O C and Woods J J 1982 The absence of neuromuscular transmission failure in sustained maximal voluntary contractions *J. Physiol.* **330** 265–78

Booghs C, Baudry S, Enoka R and Duchateau J 2012 Influence of neural adjustments and muscle oxygenation on task failure during sustained isometric contractions with elbow flexor muscles *Exp. Physiol.* **97** 918–29

Calder K M, Hall L A, Lester S M, Inglis J G and Gabriel D A 2005 Reliability of the *biceps brachii* M-wave *J. Neuroeng. Rehabil.* **6** 33

Cracco R Q and Cracco J B 1976 Somatosensory evoked potential in man: far-field potentials *Electroencephalogr. Clin. Neurophysiol.* **41** 460–6

Cupido C M, Galea V and McComas A J 1996 Potentiation and depression of the M wave in human *biceps brachii J. Physiol.* **491.2** 541–50

Dumitru D and King J C 1991 Far-field potentials in muscle *Muscle Nerve* **14** 981–9

Farina D, Fosci M and Merletti R 2002 Motor unit recruitment strategies investigated by surface EMG variables *J. Appl. Physiol.* **92** 235–47

Farina D and Negro F 2007 Estimation of muscle fiber conduction velocity with a spectral multidip approach *IEEE Trans. Biomed. Eng.* **54** 1583–9

Hunter S K, Mcneil C J, Butler J E, Gandevia S C and Taylor J L 2016 Short-interval cortical inhibition and intracortical facilitation during submaximal voluntary contractions changes with fatigue *Exp. Brain Res.* **234** 2541–51

Kameyama S, Yamada T, Matsuoka H, Fuchigami Y, Nakazumi Y, Suh C-K and Kimura J 1988 Stationary potentials after median nerve stimulation: changes with arm position *Electroericephalogr. Clin. Neitrophysiol.* **71** 348–56

Keenan K G, Farina D, Merletti R and Enoka R M 2006 Influence of motor unit properties on the size of the simulated evoked surface EMG potential *Exp. Brain Res.* **169** 37–49

Kimura J, Mitsudome A, Yamada T and Dickins Q S 1984 Stationary peaks from a moving source in far-field recording *Electroencephalogr. Clin. Neurophysiol.* **58** 351–61

Klass M, L´ev´enez M, Enoka R M and Duchateau J 2008 Spinal mechanisms contribute to differences in the time to failure of submaximal fatiguing contractions performed with different loads *J. Neurophysiol.* **99** 1096–104

Lange F, Van Weerden T W and Van Der Hoeven J H 2002 A new surface electromyography analysis method to determine spread of muscle fiber conduction velocities *J. Appl. Physiol.* **93** 759–64

Lateva Z C, Mcgill K C and Burgar C G 1996 Anatomical and electrophysiological determinants of the human thenar compound muscle action potential *Muscle Nerve* **19** 1457–68

L´ev´enez M, Garland S J, Klass M and Duchateau J 2008 Cortical and spinal modulation of antagonist coactivation during a submaximal fatiguing contraction in humans *J. Neurophysiol.* **99** 554–63

Masuda T, Miyano H and Sadoyama T 1985 The position of innervation zones in the *biceps brachii* investigated by surface electromyography *IEEE Trans. Biomed. Eng.* **32** 36–42

McFadden L K and McComas A J 1996 Late depression of muscle excitability in humans after fatiguing stimulation *J. Physiol.* **496** 851–5

Mesin L, Merletti R and Vieira T M 2011 Insights gained into the interpretation of surface electromyograms from the gastrocnemius muscles: a simulation study *J. Biomech.* **44** 1096–103

Nelson C M, Dewald J P A and Murray W M 2016 *In vivo* measurements of *biceps brachii* and *triceps brachii* fascicle lengths using extended field-of-view ultrasound *J. Biomech.* **49** 1948–52

Nelson C M, Murray W M and Dewald J P A 2018 Motor impairment-related alterations in *biceps* and *triceps brachii* fascicle lengths in chronic hemiparetic stroke *Neurorehabilit. Neural Repair* **32** 799–809

Nuzzo J L, Trajano G S, Barry B K, Gandevia S C and Taylor J L 2016 Arm posture-dependent changes in corticospinal excitability are largely spinal in origin *J. Neurophysiol.* **115** 2076–82

Ounjian M, Roy R R, Eldred E, Garfinkel A, Payne J R, Armstrong A, Toga A W and Edgerton V R 1991 Physiological and developmental implications of motor unit anatomy *J. Neurobiol.* **22** 547–59

Prutchi D 1995 A high-resolution large array (HRLA) surface EMG system *Med. Eng. Phys.* **17** 442–54

Riley Z A, Terry M E, Mendez-Villanueva A, Litsey J C and Enoka R M 2008 Motor unit recruitment and bursts of activity in the surface electromyogram during a sustained contraction *Muscle Nerve* **37** 745–53

Rodriguez-Falces J 2016 The formation of extracellular potentials over the innervation zone: are these potentials affected by changes in fibre membrane properties? *Med. Biol. Eng. Comput.* **54** 1845–58

Rodriguez-Falces J, Duchateau J, Muraoka Y and Baudry S 2015 M-wave potentiation after voluntary contractions of different durations and intensities in the tibialis anterior *J. Appl. Physiol.* **118** 953–64

Rodriguez-Falces J, Navallas J and Malanda A 2012 A new way to describe intra- and extra-cellular electrical potentials and their generation by excitable cells *Int. J. Eng. Educ.* **28** 674–85

Rodriguez-Falces J and Place N 2018a Determinants, analysis and interpretation of the muscle compound action potential (M wave) in humans: implications for the study of muscle fatigue *Eur. J. Appl. Physiol.* **118** 501–21

Rodriguez-Falces J and Place N 2018b End-of-fiber signals strongly influence the first and second phases of the M wave in the vastus lateralis: implications for the study of muscle excitability *Front. Physiol.* **9** 162

Smith J L, Martin P G, Gandevia S C and Taylor J L 2007 Sustained contraction at very low forces produces prominent supraspinal fatigue in human elbow flexor muscles *J. Appl. Physiol.* **103** 560–8

Stegeman D F, Dumitru D, King J C and Roeleveld K 1997 Near- and far-fields: source characteristics and the conducting medium in neurophysiology *J. Clin. Neurophysiol.* **14** 429–42

Thomas C K, Woods J J and Bigland-Ritchie B 1989 Impulse propagation and muscle activation in long maximal voluntary contractions *J. Appl. Physiol.* **67** 1835–42

Toia F, D'Arpa S, Brenner E, Melloni C, Moschella F and Cordova A 2015 Segmental anatomy of the vastus lateralis: guidelines for

muscle-sparing flap harvest *Plast. Reconstr. Surg.* **135** 185e–98e
Tucker K J and Türker K S 2005 A new method to estimate signal cancellation in the human maximal M-wave *J. Neurosci. Methods* **149** 31–41
van Dijk J P, Lowery M M, Lapatki B G and Stegeman D F 2009 Evidence of potential averaging over the finite surface of a bioelectric surface electrode *Ann. Biomed. Eng.* **37** 1141–51
Yamada T, Machida M, Oishi M, Kimura A and Kimura J 1985 Stationary negative potentials near the source vs positive far-field potentials at a distance *Electroencephalogr. Clin. Neurophysiol.* **60** 509–24
Zijdewind I, Butler J E, Gandevia S C and Taylor J L 2006 The origin of activity in the *biceps brachii* muscle during voluntary contractions of the contralateral elbow flexor muscles *Exp. Brain Res.* **175** 526–35

FIGURES

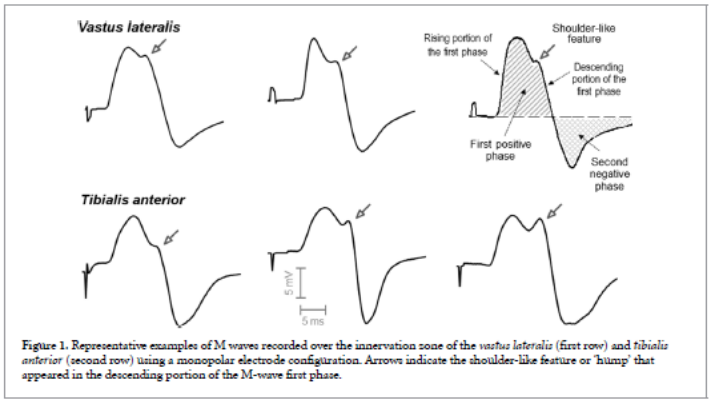

Figure 1. Representative examples of M waves recorded over the innervation zone of the *vastus lateralis* (first row) and *tibialis anterior* (second row) using a monopolar electrode configuration. Arrows indicate the shoulder-like feature or 'hump' that appeared in the descending portion of the M-wave first phase.

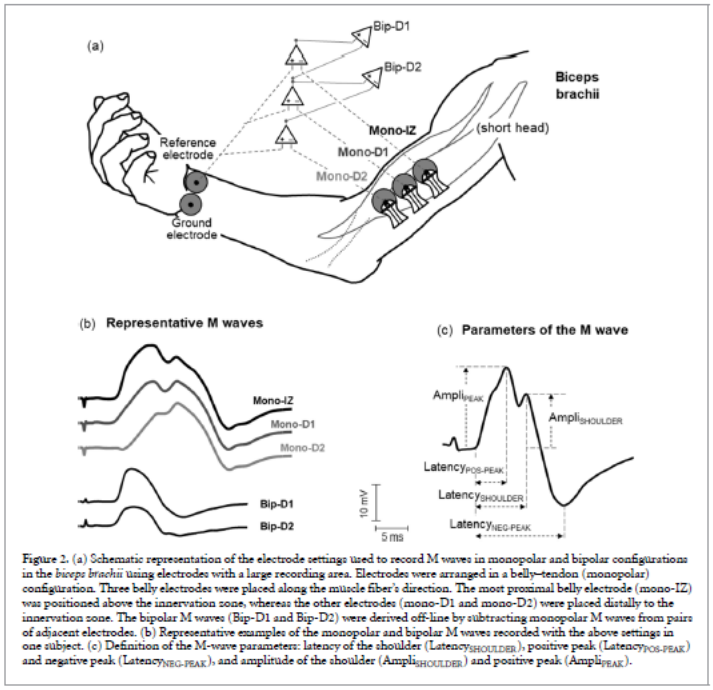

Figure 2. (a) Schematic representation of the electrode settings used to record M waves in monopolar and bipolar configurations in the *biceps brachii* using electrodes with a large recording area. Electrodes were arranged in a belly–tendon (monopolar) configuration. Three belly electrodes were placed along the muscle fiber's direction. The most proximal belly electrode (mono-IZ) was positioned above the innervation zone, whereas the other electrodes (mono-D1 and mono-D2) were placed distally to the innervation zone. The bipolar M waves (Bip-D1 and Bip-D2) were derived off-line by subtracting monopolar M waves from pairs of adjacent electrodes. (b) Representative examples of the monopolar and bipolar M waves recorded with the above settings in one subject. (c) Definition of the M-wave parameters: latency of the shoulder (Latency$_{SHOULDER}$), positive peak (Latency$_{POS-PEAK}$) and negative peak (Latency$_{NEG-PEAK}$), and amplitude of the shoulder (Ampli$_{SHOULDER}$) and positive peak (Ampli$_{PEAK}$).

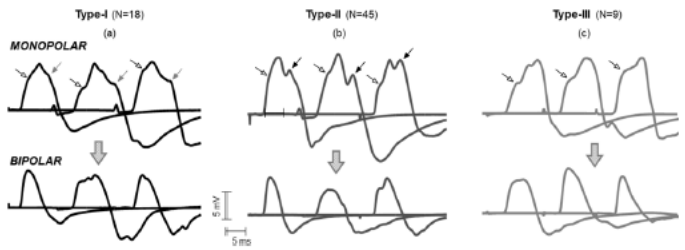

Figure 3. Representative examples of the three types of M waves identified in the *biceps brachii* (over the innervation zone) in monopolar (first row, mono-IZ) and bipolar (second row, Bip-D1) configurations. Each M wave corresponds to a different participant. N indicates the number of individuals in each category. In the type-I M waves, the descending portion of the first phase showed a shoulder-like feature (grey-headed arrow). In the type-II M waves, the shoulder is manifested by a second peak emerging in the declining first phase (black-headed arrows). The type-III M waves had a positive peak with a long latency and a declining first phase with a constant slope. In all potentials, a shoulder was also recognized in the rising portion of the first phase (white-headed arrows). For the bipolar M waves, a wide diversity of profiles was identified.

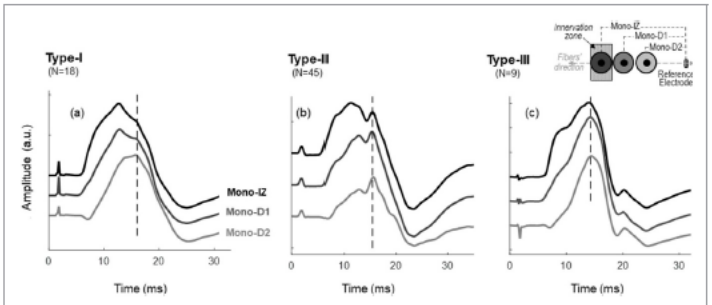

Figure 4. Representative examples of sets of M waves corresponding to the type-I (a), -II (b), and -III (c) waveforms defined in figure 3 (see text), each set comprising monopolar M waves recorded at different positions along the fibers of the *biceps brachii* from the innervation zone (mono-IZ) to the distal tendon (mono-D2).

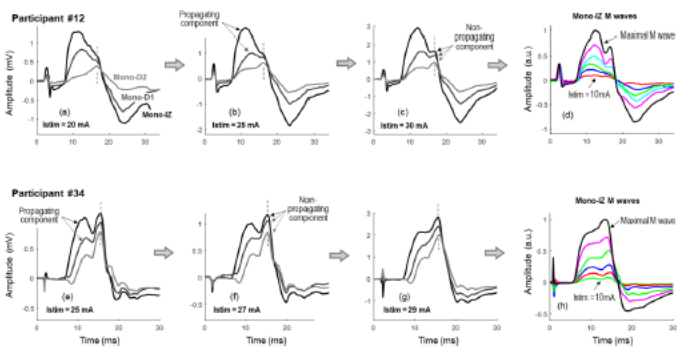

Figure 5. Representative examples of sets of M waves evoked at three submaximal stimulation intensities (Istim) for participant #12 (plots (a)–(c)) and participant #34 (plots (e)–(g)), each set comprising M waves recorded at the mono-IZ, mono-D1, and mono-D2 locations. The plots on the right side, (d) and (h), show mono-IZ M waves evoked by increasing the stimulus intensities from a subthreshold to a supramaximal level. M-wave peak amplitudes were normalised with respect to the supramaximal M wave.

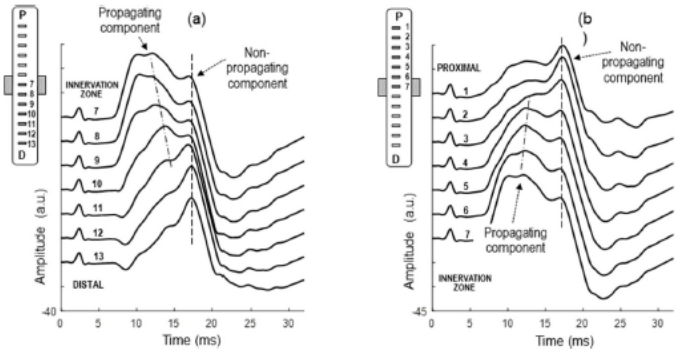

Figure 6. Representative M-wave recordings obtained from the electrode array oriented along the fiber's direction. M waves are presented in two separated sets: from the innervation zone to the distal (a) and proximal (b) tendons. Note that the second peak of the M wave had the same latency for all electrode locations.

TABLES

Table 1. Mean ± SD values of the latency of different M-wave features at different positions along the fiber's direction (mono-IZ, mono-D1, and mono-D2) for the three types of M waves identified in figure 3.

Type-I (N = 18)		Type-II (N = 45)		Type-III (N = 9)	
M-wave feature	Latency (ms)	M-wave feature	Latency (ms)	M-wave feature	Latency (ms)
Mono-IZ M wave (shoulder)	9.6 ± 0.5	Mono-IZ M wave (shoulder)	9.5 ± 0.5	Mono-IZ M wave (positive peak)	9.4 ± 0.7
Mono-D1 M wave (shoulder)	9.7 ± 0.5	Mono-D1 M wave (shoulder)	9.6 ± 0.6	Mono-D1 M wave (positive peak)	9.5 ± 0.6
Mono-D2 M wave (positive peak)	9.8 ± 0.6	Mono-D2 M wave (shoulder)	9.7 ± 0.7	Mono-D2 M wave (positive peak)	9.5 ± 0.6
Mono-IZ M wave (negative peak)	14.1 ± 1.8	Mono-IZ M wave (negative peak)	14.0 ± 1.7	Mono-IZ M wave (negative peak)	14.2 ± 1.6
Mono-D1 M wave (negative peak)	14.2 ± 1.5	Mono-D1 M wave (negative peak)	14.0 ± 1.6	Mono-D1 M wave (negative peak)	14.3 ± 1.5
Mono-D2 M wave (negative peak)	14.2 ± 1.4	Mono-D2 M wave (negative peak)	14.1 ± 1.6	Mono-D2 M wave (negative peak)	14.3 ± 1.4